The Kinematic Radial Distance

Albert Stebbins
Fermilab

Abstract

In the not too distant future we might expect that the energy dependence of time-of-arrival of neutrinos from distant supernova will become part of our cosmological dataset. Since neutrinos nave non-zero mass the arrival of lower energy neutrinos will be delayed with respect to higher energy neutrinos. This time delay provides another observable measure of distance distinct from those in common use like angular diameter (D_A) or luminosity distance (D_L). This distance measure (R_k) is dubbed the kinematic radial distance. We define R_k for arbitrary space-time geometries not limited to FLRW cosmologies or even general relativity (GR). It is shown that determining $R_k[z]$ gives distinct information about space-time geometry and in combination with $D_A[z]$ or $D_L[z]$ determines the mass distribution (in the context of GR). In practice however $R_k[z]$ is not as sensitive to general relativistic effects as other relativistic "distances" and only very precise measurements could determine the mass distribution. Allowed neutrino masses are close to being ideal for measuring R_k on cosmological scales. It is illustrated how these time delays are manifested in the observed neutrino burst and can induce flavor segregation in the observed neutrino burst.

June 15, 2012

■ Neutrinos Bursts as a Cosmological Probe

Generally speaking we have used photons to study the distant universe. These particles which move at the speed-of-light will follow null geodesics and these null geodesics only probe part of the space-time geometry. Most other particles or waves in the universe travel at very non-relativistic speeds and would not have time to travel very far over cosmological history so they are not really cosmological probes. Very high energy cosmic rays travel close to the speed of light but generally attain these high energies because they are electrically charged and this charge means that their trajectories are significantly modified by magnetic fields. Therefore charged particles are not a clean probe space-time geometry. In the past few decades we have come to realize that neutrinos have small but non-zero mass and therefore travel at nearly the speed of light even at moderate energies. As we shall see neutrino masses are close to being ideal for studying cosmology. They are not absorbed or deflected by intervening material. They do have the disadvantage of being very difficult to detect, but this can be ameliorated by using very large detectors. For cosmology especially, the bigger

Operated by Fermi Research Alliance, LLC under Contract No. De-AC02-07CH11359 with the United States Department of Energy.

the better.

There are three known neutrino flavors and therefore at least three mass eigenstates m_1, m_2, m_3. Measurements of atmospheric and solar neutrinos have shown that [1]

$$\left|m_2{}^2 - m_1{}^2\right| = \left(8.71^{+0.11}_{-0.10}\times 10^{-3}\ \mathrm{eV}\big/c^2\right)^2 \quad \left|m_3{}^2 - m_1{}^2\right| = \left(5.00^{+0.09}_{-0.16}\times 10^{-2}\ \mathrm{eV}\big/c^2\right)^2 \tag{1}$$

There is only one number missing to obtain the complete mass spectrum of neutrinos which we might hope to be determined soon. From eq. (1) one obtains a lower bound on the largest neutrino mass: Max[m_1, m_2, m_3] > $0.048\ \mathrm{eV}\big/c^2$. Laboratory measurement of inverse β-decay have limited $m_{1,}\, m_2 \lesssim 2$ eV [2]. Meanwhile somewhat model dependent cosmological measurements looking for the signature of primordial massive neutrinos indicate that the $\sum_i m_i < 0.17\ \mathrm{eV}\big/c^2$ [3] . So the maximum neutrino mass is limited to a range of less than one or two orders of magnitude depending on whether one accepts the cosmological bounds.

Supernovae (SNe) will produce bursts of neutrinos which should be readily detectable by large detectors, which has been demonstrated in the case of SN-1987a [4,5,6,7]. Gamma ray bursts (GRBs) may do the same, although at present the nature of GRBs and their neutrino spectrum is not well understood. Core collapse SNe, the most common kind, produce bursts of 10^{58} neutrinos over ~10s with energies ~10MeV [8]. In flat space the difference in arrival time between two neutrinos, a and b, emitted at the same time is [9]

$$t_a - t_b = \frac{1}{2}\left(\left(\frac{m_a}{E_a}\right)^2 - \left(\frac{m_b}{E_b}\right)^2\right)\frac{R_\mathrm{k}}{c}$$

$$= 10\ \mathrm{sec}\left(\left(\frac{m_a}{0.1\ \mathrm{eV}}\ \frac{10\ \mathrm{MeV}}{E_a}\right)^2 - \left(\frac{m_b}{0.1\ \mathrm{eV}}\ \frac{10\ \mathrm{MeV}}{E_b}\right)^2\right)\frac{R_\mathrm{k}}{2\ \mathrm{Gpc}} \tag{2}$$

where R_k is the distance to the SNe and as we shall see 2Gpc is roughly the size of our universe for the purposes of this discussion. One can measure this by comparing the arrival time of different energy or different flavor (different m_a) neutrinos. For distant enough and/or low enough energy neutrinos the different in arrival times is significantly larger than the burst length so the mass effect should be easily separable from uncertainties in the physics of SNe explosions. Unfortunately the effect is largest for the most distant SN and lowest energy neutrinos, and since neutrino flux falls off with distance and neutrino cross section falls of with decreasing energy this requires very large detectors. One would need an extremely large detector to stand a good chance of detecting even two neutrinos from a SNe at ~1Gpc, however SNe go off all the time, and one can detect these time delays statistically, even if only a small fraction of the time one detects two neutrinos from a given SNe [10].

Space is not flat on cosmological scales so a generalization of eq. (2) is required. Using neutrino time delays to determine cosmological parameters was first proposed in ref. [11,12] and we develop this idea more fully and more generally, and in the context of our present knowledge of neutrino masses and mixing. Eq. (2) is rederived for an arbitrary space-time geometry and the generalized R_k can be added to a relativist's toolkit of observable distances.

■ The Kinematic Radial Distance

Eq. (2) will be rederived in an arbitrary curved space-time to determine the meaning of R_k and what it tells us about space-time geometric. Consider the propagation of ultra-relativistic

particles from space-time events such as SN explosion to the observer here on Earth. Since the particles are ultra-relativistic they should follow geodesics which are slightly different from the null so the natural approach is a perturbation series about the null geodesics. The small variable we are expanding in is γ^{-1}, *i.e.* the inverse of the Lorentz factor in the cosmic rest frame, which is just the $m\,c^2 \big/ E$ which occurs in eq. (2).

It is perhaps easiest to do this perturbation using the "WYSWIG-T" metric formalism [13,14] which is based on observing space-time through null geodesics. The coordinates are the observation time, t, defining the past light cone, the angular position on the sky, ϑ^a, of null geodesic on the observer's past light cone connecting the observer with the distant space-time point, and a cosmic time T defined throughout space-time by the a vorticity-free velocity field of the cosmic matter flow which includes both the observer and the distant SN. Specifically the matter 4-velocity is given by $u_\mu = -c^2\, T_{,\mu}$. The observer time, t, is the cosmic time at the observer, *i.e.* $t = T_{\rm obs}$ and the metric is given by

$$d\!s^2 = -c^2\, d\!T^2 + c^2 \left(d\!T - \frac{d\!t}{1+z} \right)^2 + (d\!\boldsymbol{s}_\perp - \boldsymbol{v}_\perp\, d\!t)\cdot(d\!\boldsymbol{s}_\perp - \boldsymbol{v}_\perp\, d\!t) \tag{3}$$

where $d\!\boldsymbol{s}_\perp \cdot d\!\boldsymbol{s}_\perp = d\!\vartheta^a\, D_{ab}\, d\!\vartheta^b$, $\boldsymbol{v}_\perp \cdot d\!\boldsymbol{s}_\perp = \dot{\vartheta}^a\, D_{ab}\, d\!\vartheta^b$, $\boldsymbol{v}_\perp \cdot \boldsymbol{v}_\perp = \dot{\vartheta}^a\, D_{ab}\, \dot{\vartheta}^b$, $z[t,\, T,\, \vartheta^a]$ is the redshift of the distant point as seen by the observer, $D_{ab}[t,\, T,\, \vartheta^a]$ is a 2×2 matrix encodes information about gravitational lensing including the angular diameter distance, and $\dot{\vartheta}^a[t,\, T,\, \vartheta^a]$ is the proper motion of the matter as seen by the observer. By definition, at the observer $T = t$ and $z[t,\, t,\, \vartheta^a] = 0$. The $d\!\boldsymbol{s}_\perp$ and $\boldsymbol{v}_\perp$ are 2-vectors perpendicular to the line-of-sight representing the incremental transverse distance and transverse velocity of the matter wrt a point of constant angular position, respectively. For the purpose of this paper the most important thing is that lines-of-sight (meaning null geodesics which intersect the world line of the observer) are simply lines of constant t and ϑ^a.

If we use cosmic time, T, to parameterize an arbitrary geodesic instead of the usual affine parameter the geodesic curve is

$$\tilde{x}^\mu[T] = \left\{ \tilde{t}[T],\, \tilde{T}[T],\, \tilde{\vartheta}^a[T] \right\} \tag{4}$$

(the tildes indicate objects evaluated on the geodesic curve) while the geodesic equation is

$$\ddot{\tilde{x}}^\mu + \left(\tilde{\Gamma}^\mu_{\nu\xi} - \dot{\tilde{x}}^\mu\, \tilde{\Gamma}^T_{\nu\xi} \right) \dot{\tilde{x}}^\nu\, \dot{\tilde{x}}^\xi = 0 \qquad \tilde{\Gamma}^\mu_{\nu\xi}[T] = \Gamma^\mu_{\nu\xi}[\tilde{x}^\eta[T]]. \tag{5}$$

where $\Gamma^\mu_{\nu\xi}$ is the Christoffel symbol and over dots indicates derivatives wrt T.

Since $\tilde{T}[T] = T$ we know $\ddot{\tilde{T}} = 0$ and $\dot{\tilde{T}} = 1$. Next consider a central geodesic, $\tilde{x}^\mu_{(0)}[T]$, and neighboring geodesics $\tilde{x}^\mu_{(0)}[T] + \delta\, \tilde{x}^\mu[T]$. $\tilde{x}^\mu_{(0)}[T]$ must be as solution to eq. (5). Expanding the geodesic equation to 1st order in $\delta\, \tilde{x}^\mu$ it becomes

$$\begin{aligned} &\delta\, \ddot{\tilde{x}}^\mu - \left(\tilde{\Gamma}^T_{\nu\xi}\, \dot{\tilde{x}}^\nu_{(0)}\, \dot{\tilde{x}}^\xi_{(0)} \right) \delta\, \dot{\tilde{x}}^\mu + \\ &\quad 2 \left(\tilde{\Gamma}^\mu_{\nu\eta}\, \dot{\tilde{x}}^\nu_{(0)} - \dot{\tilde{x}}^\mu_{(0)}\, \tilde{\Gamma}^T_{\nu\eta}\, \dot{\tilde{x}}^\nu_{(0)} \right) \delta\, \dot{\tilde{x}}^\eta + \left(\tilde{\Gamma}^\mu_{\nu\xi,\eta}\, \dot{\tilde{x}}^\nu_{(0)}\, \dot{\tilde{x}}^\xi_{(0)} - \dot{\tilde{x}}^\mu_{(0)}\, \tilde{\Gamma}^T_{\nu\xi,\eta}\, \dot{\tilde{x}}^\nu_{(0)}\, \dot{\tilde{x}}^\xi_{(0)} \right) \delta\, \tilde{x}^\eta = 0 \end{aligned} \tag{6}$$

where $\tilde{\Gamma}^\mu_{\nu\xi}[T] = \Gamma^\mu_{\nu\xi}\left[\tilde{x}^\mu_{(0)}[T]\right]$ and $\tilde{\Gamma}^\mu_{\nu\xi,\eta}[T] = \Gamma^\mu_{\nu\xi,\eta}\left[\tilde{x}^\kappa_{(0)}[T]\right]$ and $\delta\, \tilde{x}^T = 0$. Now specialize to the case where $\tilde{x}^\mu_{(0)}[T]$ is a line-of-sight so that $\dot{\tilde{x}}^\mu_{(0)}[T] = \{0,\, 1,\, 0,\, 0\}$. Noting that

$\Gamma^t_{tT} = \Gamma^t_{Tt} = \Gamma^t_{TT} = \Gamma^t_{Ta} = \Gamma^t_{aT} = \Gamma^a_{TT} = 0$ in WYSWYG-T coordinates the perturbed geodesic equations become

$$\ddot{\delta\tilde{t}} - \tilde{\Gamma}^T_{TT}\,\dot{\delta\tilde{t}} = 0 \tag{7}$$

$$\ddot{\delta\tilde{\vartheta}}^a - \tilde{\Gamma}^T_{TT}\,\dot{\delta\tilde{\vartheta}}^a + 2\,\tilde{\Gamma}^a_{Tt}\,\dot{\delta\tilde{t}} + 2\,\tilde{\Gamma}^a_{Ta}\,\dot{\delta\tilde{\vartheta}}^a = 0$$

The unperturbed line-of-sight must connect the SN at $\{t_*, T_*, \vartheta^a_*\}$ with the observer at $\{t_*, t_*, \vartheta^a_*\}$. If we want to describe massive particles coming from the same event they also must connect $\{t_*, T_*, \vartheta^a_*\}$ with the central observer but are observed at some different observation time and possibly coming from some other direction, i.e. $\{t_*, t_* + \delta t_*, \vartheta^a_* + \delta\vartheta^a_*\}$.

This corresponds to boundary conditions $\delta\tilde{t}[0] = \delta t_*$, $\delta\tilde{t}[T_*] = 0$, $\delta\tilde{\vartheta}^a[T_*] = 0$, and $\dot{\delta\tilde{\vartheta}}^a[0] = 0$. If the last condition is not satisfied the geodesic would miss the observer entirely. Thus we see we have a one parameter family of geodesics parameterized by δt_*. We expect massive particles to travel on time-like geodesics so we expect the perturbed geodesic to arrive *after* the null geodesic, *i.e.* $\delta t_* \geq 0$. Observing $\delta t_* < 0$ would indicate a space-like geodesic or superluminality.

The equation for $\delta\tilde{t}[T]$ is not coupled to the equation for $\delta\tilde{\vartheta}^a$ so we may solve it separately. What this means is that to 1st order we can think of the massive particle as following the same path as the massless particle but delayed in time. One can derive from eq. (3) that $\tilde{\Gamma}^T_{TT} = -\frac{\partial \ln[1+z]}{\partial T}$ so with the boundary conditions we find the solution

$$\delta\tilde{t}[T] \propto \int_{T_*}^{T} \frac{dT}{1 + z[t, T, \vartheta^a]} \tag{8}$$

A separate boundary conditions at the observer is $\dot{\delta\tilde{t}} = 1 - \frac{v}{c} \cong \frac{1}{2\,\gamma_{\rm obs}{}^2} = \frac{1}{2}\left(\frac{m}{E_{\rm obs}}\right)^2$ where v and $\gamma_{\rm obs}$ are respectively the speed and Lorentz factor of the particle when it arrives as the observer, whereas $E_{\rm obs}$ and m are the particle's total energy and mass. So one can write

$$\delta\tilde{t}_{\rm obs} = \frac{1}{2}\left(\frac{m\,c^2}{E_{\rm obs}}\right)^2 \frac{R_{\rm k}}{c}\left(1 + O\left[\gamma_{\rm obs}{}^{-1}\right]\right) \tag{9}$$

where the *kinematic radial distance*, $R_{\rm k}$, is defined by the line-of-sight integral

$$R_{\rm k}[t_{\rm obs}, z, \vartheta^a] \equiv c \int_{T_*}^{t_{\rm obs}} \frac{dT}{1 + z[t_{\rm obs}, T, \vartheta^a]}. \tag{10}$$

which will depend on the time of observation, t, and the redshift and direction, z, and ϑ^a, of the source. Recall that $\delta\tilde{t}_{\rm obs}$ is defined to be the difference in time of arrival of massive particles and massless particle emitted at the same time and from the same place and the cosmic time T is the time defined by the rest frame of *any* vorticity free velocity flow which is comoving with both the emission and observation event. Eq. (9) validates the generalization of the flat space formula, eq. (2), to an arbitrary spacetime, when the $R_{\rm k}$ is defined as in eq. (10). The adjective *radial* is used in the name because $R_{\rm k}$ is more directly a measure distance along the line-of-sight (radius) than other distances like the angular diameter distance which are more properly apparent distances. Note that $R_{\rm k}$ is defined to be the term that gives $\delta\tilde{t}_{\rm obs}$ to leading order in $\gamma_{\rm obs}{}^{-1}$ and higher order corrections will give

different information about the space-time geometry.

A more intuitive expression for R_k can be gotten by noting that the difference in speeds between a massive and massless particle is $c - v \cong \frac{1}{2}\gamma^{-2} \cong \frac{1}{2} c\, \gamma_{obs}{}^{-2} (1+z)^{-2}$ so that eq. (9) can be rewritten

$$\frac{\delta \tilde{t}_{obs}}{c} \cong \int_{T_*}^{t_{obs}} dT\, (c - v)\, (1+z) \tag{11}$$

where $\delta \tilde{x}_{obs} = \delta \tilde{t}_{obs} / c$ is the spatial separation between the faster in slower particle in the observer frame at the observer. This formula tells us that in the matter frame the rate of growth of the spatial separation between the faster and slower particle is $c - v$ and this must be multiplied by a redshift factor $1 + z$ since changes in redshift will grow or shrink this separation.

■ Proper Time-Of-Flight

In the cosmic frame the Lorentz factor for ultra-relativistic particle is $\tilde{\gamma}[T] \cong \gamma_{obs}(1+z)$. Thus the proper time-of-flight which is experienced by the particle between the emission and the observation is given by the Lorentz factor of the geodesic in the matter frame:

$$\tau_{tof}[t_{obs}, z, \vartheta^a] = \int_{T_*}^{t_{obs}} \frac{dT}{\tilde{\gamma}[T]} \cong \frac{1}{\gamma_{obs}} \int_{T_*}^{t_{obs}} \frac{dT}{1 + z[T]} = \frac{R_k[t_{obs}, z, \vartheta^a]}{c\, \gamma_{obs}}. \tag{12}$$

Thus R_k not only gives us the time delay but also the proper time-of-flight, something which is particularly relevant for unstable particles with known half-life. From this we see that the proper time-of-flight is roughly the geometric mean of the time delay and the kinematic radial distance, *i.e.*

$$\tau_{tof} = \sqrt{2\, \delta \tilde{t}_{obs}\, R_k / c} \tag{13}$$

Thus for cosmological distances of billions of light years and time delays of 10s of seconds the proper time-of-flight is decades.

Another neutral particle which one might consider applying this method to is neutrons, which are unstable with lifetime of 886 sec. We see however that in order to for the neutrons to survive with $R_k \sim 10^9$ light years it would require energies of $E_n \gtrsim 10^{23}$ eV which is much greater than the GZK cutoff [15,16] above which the universe is opaque to ultra-high energy cosmic rays because of collisions with diffuse light.

■ Other Distances

In metric theories one can devise other observable distance measures [17,18] to events on ones past light cone. The most commonly used in theory is the angular diameter distance

$$D_A \equiv \frac{\text{transverse physical size}}{\text{angular size (radians)}}. \tag{14}$$

while in practice the most commonly used is the (bolometric) luminosity distance

$$D_{\rm L} \equiv \sqrt{\frac{\text{absolute bolometric luminosity}}{\text{apparent bolometric luminosity}}} = (1+z)^2\, D_{\rm A}. \tag{15}$$

As one adds more features to the space-time one can construct more distances. We have, for convenience, used a velocity field, $u_\mu = -c^2\, T_{,\mu}$ to write down an expression for $R_{\rm k}$ although the meaning of $R_{\rm k}$ is independent on which time function, T, one chooses. However if there really is a physically defined irrotational matter velocity we can define a lookback distance

$$R_{\rm lb} \equiv t_{\rm obs} - T_* \tag{16}$$

which does depend on the physically defined time function T which is used. Also there can be a well defined comoving distance, such as might be determined by the separation of features in the distribution of matter comoving with u_μ (such as baryon acoustic oscillations, BAOs). One can define the radial comoving distance as the integral of the increments of comoving distance along the line-of-sight

$$R_{\rm co} \equiv \int d\!\!\!/ R_{\rm co} \tag{17}$$

and one can also define a comoving angular diameter, $D_{\rm A,co}$, which is

$$D_{A,\rm co} \equiv \frac{\text{transverse comoving size}}{\text{angular size (radians)}} = (1+z)\, D_{\rm A}. \tag{18}$$

All of these are distinct measures of distance.

The universe is usually studied under the assumption of the Cosmological Principle meaning the space-time is approximately homogeneous and isotropic about each point and is described by a Friedman-Lemaitre-Robertson-Walker (FLRW) space-time. This metric defines a cosmic time T which delineates 3-surfaces of spatial homogeneity. By symmetry the matter must flow with the 4-velocity $u_\mu = -c^2\, T_{,\mu}$. The evolution of the space-time is described by a scale factor $a[T]$ and the redshift of the matter is $z[T] = \frac{a[t_{\rm obs}]}{a[T]} - 1$. The Hubble expansion rate is $H = \frac{\dot a[T]}{a[T]} = -\frac{\dot z[T]}{1+z[T]}$ and is usually expressed as a function of the observable redshift z. Normalizing the comoving distances to coincide with the physical distances at $z = 0$ one can write the various distances as

$$R_{\rm lb}[z] = c\int_0^z \frac{dz}{(1+z)\,H[z]} \qquad D_{A,\rm co}[z] = \begin{cases} \frac{\mathrm{Sin}\left[\sqrt{K}\; R_{\rm co}[z]\right]}{\sqrt{-K}} & K > 0 \\ R_{\rm co}[z] & K = 0 \\ \frac{\mathrm{Sinh}\left[\sqrt{-K}\; R_{\rm co}[z]\right]}{\sqrt{-K}} & K < 0 \end{cases} \qquad D_{\rm A}[z] = \frac{1}{1+z}\, D_{A,\rm co}[z] \tag{19}$$

$$R_{\rm co}[z] = c\int_0^z \frac{dz}{H[z]} \qquad D_{\rm L}[z] = (1+z)\, D_{A,\rm co}[z] \qquad R_{\rm k}[z] = c\int_0^z \frac{dz}{(1+z)^2\, H[z]}$$

where $H_0 \equiv H[z=0]$ and $K = \left(\frac{H_0}{c}\right)^2 (\Omega_0 - 1)$ is the spatial curvature at $z = 0$ and Ω_0 is the density parameter. This expression for $R_{\rm k}[z]$ is a restatement of eq. (10) for FLRW spacetime

and can also be found in ref. [12]. Note that in an FLRW space-time all of these distances are related to each other through $H[z]$ and Ω_0.

One can describe the space-time geometry of our universe on large scales by an FLRW cosmology with matter (dark matter + baryons), radiation, and dark energy with a Dark Energy Task Force equation-of-state dark $p_{\rm DE} = \rho_{\rm DE}\, c^2(a\, w_0 + (1-a)\, w_{\rm i})$ [19] where $a = \frac{1}{1+z}$ is the scale factor and the Hubble parameter is thus

$$H[z] \cong H_0 \sqrt{\left(\frac{1-\Omega_0}{a^2} + \frac{\Omega_{\rm m0}}{a^3} + \frac{\Omega_{\rm r,0}}{a^4} + \frac{\Omega_0 - \Omega_{\rm m,0} - \Omega_{\rm r,0}}{a^{3\,(1+w_{\rm i})}}\, e^{3\,(w_0 - w_{\rm i})\,(1-a)} \right)} \tag{20}$$

The parameters and measured values [20] are the Hubble constant, $H_0 \cong 71\,{\rm km/sec/Mpc}$, the density parameter $\Omega_0 \cong 1$, the matter density parameter $\Omega_{\rm m0} \cong 0.27$, the radiation density parameter, $\Omega_{\rm r0} \cong 8.3\times 10^{-5}$, and the dark energy equation of state parameter $w \cong -1$. By definition the dark energy density parameter is $\Omega_{\rm DE0} \equiv \Omega_0 - \Omega_{\rm m0} - \Omega_{\rm r0} \cong 0.73$. In figure 1 we plot the various measures of distance as a function of redshift for this concordance cosmology (since $\Omega_0 = 1$ $R_{\rm co}[z] = D_{A,{\rm co}}[z]$ and there are not separate curves for these). At lo-z we are in the flat space limit and they all concur. We see that compared to the other distances $R_{\rm k}[z]$ "saturates" at a fairly low z reaching a maximum of only $R_{\rm k}[\infty] = 2.3\,{\rm Gpc}$ in contrast with $R_{\rm lb}[\infty] = 4.39\,{\rm Gpc}$ and $R_{\rm co}[\infty] = D_{A,{\rm co}}[\infty] = 14.9\,{\rm Gpc}$. All SNe at high redshift, say $z > 1$, which is the vast majority of SNe, will have nearly the same kinematic radial distance: $R_{\rm k} \in 2.03 \pm 0.27\,{\rm Gpc}$. This is indicative of the fact that $R_{\rm k}[z]$ is mostly sensitive to the cosmology at low redshifts. One can quantify the sensitivity to parameters in a rough way by computing the variation of $R_{\rm k}[z=\infty]$ with parameter changes at the measured parameter values:

$$\begin{pmatrix} d\ln[R_{\rm k}[\infty]] \\ d\ln[R_{\rm lb}[\infty]] \\ d\ln[R_{\rm co}[\infty]] \end{pmatrix} =$$

$$\begin{pmatrix} -1 & +0.308 & -0.197 & -0.000166 & -0.183 & -0.0362 \\ -1 & +0.345 & -0.274 & -0.000428 & -0.171 & -0.0398 \\ -1 & +0.269 & -0.392 & -0.009822 & -0.097 & -0.0272 \end{pmatrix} \begin{pmatrix} d\ln[H_0] \\ d\ln[\Omega_0] \\ d\ln[\Omega_{\rm m0}] \\ d\ln[\Omega_{\rm r0}] \\ d\,w_0 \\ d\,(w_{\rm i} - w_0) \end{pmatrix} \tag{21}$$

We see that $R_{\rm k}$ has sensitivity to most parameters comparable to that of $R_{\rm lb}$ or $R_{\rm co}$, with the exception that it has much lower sensitivity to $\Omega_{\rm r0}$ which describes the very early universe.

If one knew the absolute distance to a SN one could determine the absolute neutrino mass by measuring the time delays. Conversely if one knew the neutrino masses then a measure of the time delay tells us $R_{\rm k}$ directly, completely skipping the cosmological distance ladder [18]. In contrast SNe-Ia surveys which measure $D_{\rm L}[z]$, large-scale structure surveys which measure $R_{\rm co}[z]$ and $D_{A,{\rm co}}[z]$, and cosmic microwave background temperature anisotropy mapping which determines $D_{\rm A}[z_{\rm rec}]$ all require some knowledge of H_0 to translate their measurements

to physical distances. Even if we don't currently have absolute measurements of neutrino masses we see that the measured laboratory mass differences are sufficient to determine the relative time delays of two neutrinos in different mass eigenstates. Cosmological probes of neutrino masses can determine the absolute neutrino mass scale independently of the cosmic distance ladder [18], while a nearby SN could also do so in a way which skips much of distance ladder.

■ Determining the Stress-Energy Directly

In an FRW spacetime knowledge of any one distance function, $D[z]$, plus one number is sufficient to determine $H[z]$ and Ω_0 which completely determines the space-time geometry and using Einstein's equations the stress energy of all the matter. In place of the one number one could use a different distance function. So for example BAO surveys which measure $R_{\rm co}[z]$ and $D_{A,{\rm co}}[z]$ completely determines the space-time apart from a normalization of scale which requires knowledge of H_0. However this requires the assumption of the Cosmological Principle. The construction of any measure of comoving distance, such as BAO's, requires the assumption of homogeneity.

As pointed out in ref. [14] one can more directly measure space-time geometry if one supplements $D_{\rm A}[z]$ or $D_{\rm L}[z]$ with a direct measure of the radial distance. The kinematic radial distance is one such measure, the lookback distance is another. In particular in any space-time along every line-of-sight

$$\frac{\left(\frac{D'_{\rm A}}{R'_{\rm k}}\right)' \frac{R'_{\rm k}}{D_{\rm A}} + \frac{1}{4}\,\frac{\Gamma'^2}{1+\Gamma^2} + \alpha'^2\,\Gamma^2}{(1+z)^2\,R'^2_{\rm k}} = -\,\frac{1}{2}\,n^\mu\,n^\nu\,R_{\mu\nu} = -\,\frac{4\,\pi\,G}{c^4}\,n^\mu\,n^\nu\,T_{\mu\nu} = -\,\frac{4\,\pi\,G}{c^2}\left(\rho + \frac{p}{c^2}\right) \tag{22}$$

where $'$ is a derivative with respect to z, Γ is the reduced shear as measured by lensing, α is the position angle of the shear (in radians), $R_{\mu\nu}$ is the Ricci curvature tensor, $T_{\mu\nu}$ the stress-energy and n^μ is the null vector along the line-of-sight normalized such that $n^\mu\,u_\mu = c$ where u_μ is the 4-velocity of the matter which defines the redshift. The 1st equality applies to any metric theory of gravity in which the light and matter are free-falling while the 2nd equality assumes Einstein's equations, and the third equality holds if the stress-energy takes a perfect fluid form with 4-velocity u_μ, i.e. $T_{\mu\nu} = \left(\rho + p\,/\,c^2\right)u_\mu\,u_\mu + p\,g_{\mu\nu}$. Note that the contribution of a cosmological constant, $p = -\rho\,c^2$ to the right-hand-side of eq. (22) is zero. Thus in a ΛCDM model where there is only a cosmological constant (Λ) and "matter" ($|p| \ll |\rho|\,c^2$) eq. (22) determines only the distribution of the matter.

Define at each point $H_{\rm II} \equiv \frac{c}{(1+z)^2\,R'_{\rm k}}$, which is the matter frame line-of-sight velocity gradient or Hubble parameter; an effective density parameter, $\Omega_{\rm II} \equiv \frac{8\,\pi\,G\,\rho}{3\,H_{\rm II}^{\,2}}$; and an equation-of-state parameters, $w \equiv \frac{p}{\rho\,c^2}$. Then in any geometry at every point along all lines-of sight eq. (22) reads

$$\left(\frac{D'_{\rm A}}{R'_{\rm k}}\right)' \frac{R'_{\rm k}}{D_{\rm A}} + \frac{1}{4}\,\frac{\Gamma'^2}{1+\Gamma^2} + \alpha'^2\,\Gamma^2 = -\,\frac{3}{2}\,\frac{\Omega_{\rm II}\,(1+w)}{(1+z)^2} \tag{23}$$

These equations are exact and non-perturbative and hold whether or not the Cosmological Principal is true. If one had precision measurements of D_A, R_k, Γ, and α with dense redshift coverage one could use this equation to map out the redshifts space distribution of H_{II}, $\rho + \frac{p}{c^2}$ and/or $\Omega_{II}\,(1 + w)$ on your past light cone.

The gravitational lensing terms, Γ and α, are known to be small, $\Gamma \lesssim 10^{-2}$ and subdominant for most lines-of-sight. It is curious that the dominant term on the right-hand-side, D_A and R_k, are likely both obtained from SNe, D_A from Type Ia SNe and R_k predominantly from Type II core collapse SNe.

It will not be easy to obtain such precision measurements with dense sampling. One can average this equation over redshift space volumes since it is true at every point. Since detecting SN neutrinos and hence measuring R_k is increasingly difficult with increasing redshift one would start at small redshift where the lensing term goes to zero. So long as $|\Omega_{II}\,(1 + w)|_{z=0} < \infty$, then $R_k = D_A = 0$, $R_k' = D_A' = c\,/\,H_{II}$, and $R_k'' = D_A'' = -c\,H_{II}'\,\big/\,H_{II}^{\,2}$ at $z = 0$ so

$$\Omega_{II}\,(1 + w)|_{z=0} \;=\; \frac{2}{3}\,\frac{H_{II}}{c}\,(R_k''' - D_A''')\Big|_{z=0} \tag{24}$$

Thus one needs to accurately measure third redshift derivatives of distances to determine $\Omega_{II}\,(1 + w)$ at low redshift from eq. (23). The flip side of this is that at low redshifts the kinetic radial distance is an accurate surrogate for the angular diameter distance:

$$D_A = R_k \;-\; \frac{1}{4}\,\frac{c}{H_{II}}\,\Omega_{II}\,(1 + w)\Big|_{z=0} z^3 + O\big[z^4\big] \tag{25}$$

as is apparent in figure 1 for a concordance cosmology where the two are nearly indistinguishable up to $z \approx 0.6$. The agreement between these two distance measures is one power of z better than is typical. One could use this, for example, to obtain the distribution of absolute luminosities of SN by measuring their apparent luminosities and R_k.

■ Neutrino Bursts and Flavor Segregation

While we have indicated that differential time delays can be used to measure the kinematic radial distance we have been a bit vague how this would work in practice. Here we attempt to illustrate the effect graphically and clarify how flavor oscillations come into play. It is well established that neutrinos oscillate between flavors which is another consequence of the varying mass eigenstates and the origin of the experimental results listed in of eq. (1).

Assuming three neutrino flavors the neutrino mass matrix is

$$\boldsymbol{\mathcal{M}} = \boldsymbol{U}\cdot\begin{pmatrix} m_1 & 0 & 0 \\ 0 & m_2 & 0 \\ 0 & 0 & m_3 \end{pmatrix}\cdot\boldsymbol{U}^{\mathrm{T}} \qquad \boldsymbol{U} = \begin{pmatrix} U_{e1} & U_{e2} & U_{e3} \\ U_{\mu 1} & U_{\mu 2} & U_{\mu 3} \\ U_{\tau 1} & U_{\tau 2} & U_{\tau 2} \end{pmatrix} \cong \begin{pmatrix} +0.820 & +0.552 & +0.153 \\ -0.479 & +0.513 & +0.713 \\ +0.315 & -0.658 & +0.684 \end{pmatrix} \tag{26}$$

where $\boldsymbol{U}$ is the unitary Pontecorvo-Maki-Nakagawa-Sakata matrix, and the last expression is gotten by taking the best experimental values (universal fit) to the neutrino mixing angles [1] augmented by the recent Daya Bay measurement of θ_{13} [10], and by setting the CP violating

phases to zero, which is consistent with current data. This means that there is no oscillation between neutrinos and anti-neutrinos and $\boldsymbol{U}$ is real and orthogonal.

The neutrino flux of flavor α at the Earth in particles per unit area per unit energy per unit time (observer frame) is given by

$$F_\alpha[E_\nu, t] = \frac{1}{D_{\mathrm{A}}{}^2} \sum_{i=1}^{3} U_{\alpha i}{}^2 \sum_{\beta=1}^{3} U_{\beta \mathrm{i}}{}^2 \mathcal{F}_\beta\left[(1+z)\, E_\nu,\ \frac{t - \frac{R_{\mathrm{lb}}}{c} - \frac{1}{2}\left(\frac{m_i\, c^2}{(1+z)\, E_\nu}\right)^2 \frac{R_k}{c}}{1+z}\right] \tag{27}$$

in terms of $\mathcal{F}_\beta[E_\nu, t]$ which is the neutrino flux of flavor β in particles per unit solid angle per unit energy per unit time (SN frame) emitted toward the Earth from the SN in the SN frame. The time arguments of F_α and $\mathcal{F}_\beta$ are the cosmic time at the Earth and SN respectively. These two times are separated by a very large interval, the "lookback time" or "cosmic time-of-flight" $t_{\mathrm{lb}} = R_{\mathrm{lb}} / c$, but since we have no *a proiri* knowledge of the time of an explosion t_{lb} is not an observable. Nevertheless it is interesting to see that three distance measures, D_{A}, R_{lb}, and R_k enters this expression.

Eq. (27) is obtained by averaging over flavor oscillations which at cosmic distances are extremely rapid functions of energy and essentially unobservable. It is written as if neutrinos are emitted (or last scattered) in flavor eigenstates which may or may not be the case. What really matters is the number of neutrinos which end up in different mass eigenstates which is given by the subexpression, $\mathcal{F}_i[E_\nu, t] = \sum_{\beta=1}^{3} U_{\beta \mathrm{i}}{}^2 \mathcal{F}_\beta[E_\nu, t]$. Since U is orthogonal $\sum_{\beta=1}^{3} U_{\beta \mathrm{i}}{}^2 = \sum_{i=1}^{3} U_{\alpha i}{}^2 = 1$ so $D_{\mathrm{A}}{}^2 F_\alpha$ is a weighted average of the different mass fluxes, $\mathcal{F}_i$, which in turn is a weighted average of the different flavor fluxes, $\mathcal{F}_\beta$.

In figures 2&3 we plot the neutrino burst profiles at Earth as a function of time and energy for a simplistic initial profile, and for a variety of distance and neutrino mass scenarios. In many cases the effect of non-zero neutrino masses is obvious to the eye as a bend in the low energy tail. In some of these cases at low energies there is a clear separation in time between the $m_1 + m_2$ pulse and m_3 pulse as a split into a two colored tail, which is here called *flavor segregation*. Note we are Assuming no flavor segregation in the initial pulse. Many modes of neutrino detection, those involving charged current interactions, are only sensitive to electron neutrinos which contain only a small admixture of m_3 and would not be sensitive to the blue-green tail. Neutral current interactions are sensitive to all flavors and could in principle see both pulses. However the $m_1 + m_2$ pulse, involving two mass eigenstates, is likely to be twice as strong as the m_3 pulse involving only one.

The third column of figure 3 illustrates the effect of redshift which causes the neutrino burst energy to decrease and it's burst length (in observer time) to dilate. Determining the time-of-arrival of neutrino events accurately is not technically challenging. The largest systematic error in measuring the time delays is uncertainties in the burst shape. One would expect the size of this systematic goes like the ratio of the time delay $\propto R_{\mathrm{k}}\, E_\nu{}^{-2} \propto R_{\mathrm{k}}[z]\,(1+z)^2$ to the Earth frame burst length $\propto (1+z)$. So a systematic figure of merit for measuring the time delays might be

$$\left|\frac{\delta \mathrm{R_k}}{R_\mathrm{k}}\right|_\mathrm{sys} \propto \frac{\delta\, \tilde{t}_\mathrm{obs}}{\delta \mathrm{t_{SN}}} \propto R_\mathrm{k}[z]\,(1+z) \tag{28}$$

which increases with distance as is obvious in figures 1&3. A far more important effect is the statistical error associated with the numbers of neutrinos detected. The neutrino flux at Earth decreases as $D_\mathrm{A}{}^{-2}$, but it is worse than that, since the weak interaction cross-sections are an increasing function of energy, so the redshifting of neutrino energy leads to fewer neutrinos detected. This is exacerbated by the increasing backgrounds at lower energies from solar and reactor neutrinos and other sources of radioactivity as well as the degradation of energy resolution at low energies. While the neutrino bursts in figures 2 & 3 extend down to $E_\nu = 0.1\,\mathrm{MeV}$ one usually considers detecting SNe neutrinos at $E_\nu > 10\,\mathrm{MeV}$. However sub-MeV neutrino astronomy is possible in practice [22] although non-solar applications must contend with large backgrounds from solar and reactor neutrinos in addition to local radioactivity. Optimistically, the only non-ameliorable problem is the decreasing weak interaction cross-section which scales like $\sigma_\mathrm{w} \sim G_\mathrm{F}{}^2\, E_\nu{}^2 \big/ \left(2\,\pi\,(\hbar\, c)^4\right)$ [a]. The total number of neutrinos which goes through a detector scales $\propto D_\mathrm{A}{}^{-2}$ however due to the redshifted energy the number of neutrinos detected (under these optimistic assumptions) scales $\propto D_\mathrm{A}{}^{-2}\,(1+z)^{-2}$.

One would expect that any statistical errors associated with low neutrino counts scales like the square root of the number of neutrinos detected. Thus one would expect the statistical error to scale like

$$\left|\frac{\delta \mathrm{R_k}}{R_\mathrm{k}}\right|_\mathrm{stat} = 2\,\frac{\delta \mathrm{m}_\nu}{m_\nu} \propto \sqrt{\#_\nu}\,\frac{\delta\, \tilde{t}_\mathrm{obs}}{\delta \mathrm{t_{SN}}} \propto \frac{R_\mathrm{k}[z]\,(1+z)}{D_\mathrm{A}[z]\,(1+z)} = \frac{R_\mathrm{k}[z]}{D_\mathrm{A}[z]} \underset{z \lesssim 1}{\cong} 1. \tag{29}$$

For fixed neutrino masses and integrated neutrino flux, shorter bursts (smaller $\delta \mathrm{t_{SN}}$) are better. It is shown elsewhere that features in SN burst profile with smaller timescales than the total burst length will determine $\delta \mathrm{t_{SN}}$ [10]. It was shown above that at small redshift, $R_\mathrm{k}[z] \cong D_\mathrm{A}[z]$, so this equation suggests the incredible (pun intended) result that the statistical errors in determining $R_\mathrm{k}[z]$, from single SN by a fixed detector, is independent of distance (out to $z \approx 1$). The reason this formula is not fully credible is that $\#_\nu$ is an integer and one learns nothing about R_k if 0 or 1 neutrinos is detected. So eq. (29) does not apply unless multiple neutrinos are detected from the SN [b]. The proper interpretation of eq. (29) is that for a given detector there is a distance range, $D_\mathrm{A}^\mathrm{range}$, below which the fractional errors on R_k or m_ν are independent of distance. If $D_\mathrm{A}^\mathrm{range}$ extends to extra-Galactic SNe then the extra-Galactic SN gives just as much information regarding neutrino-masses or SN distances as a Galactic SN! Since the SN rate increases with volume, scaling even faster than the volume, $\gtrsim D_\mathrm{A}{}^3$, due to the decreasing star formation rate with time, the information rate about distances and neutrino masses are dominated by the most distant SNe accessible by your detector! One might naively think that the infrequent Galactic SN would give the most information about neutrino masses, but for large detectors this is not the case. However a Galactic SN would help to calibrate the neutrino burst profile and thus greatly decrease systematic errors.

Now let us review some, well known, quantitative aspects of SN neutrino detection. A SN emits $\sim 10^{58}$ neutrinos with mean energy $\sim 20\,\mathrm{MeV}$ [8] so the number of neutrinos detected

scales like

$$\sharp_\nu \approx \frac{10^{58}}{2\,\pi}\,\frac{G_{\rm F}{}^2\,(20\,{\rm MeV})^2}{D_{\rm A}[z]^2\,(1+z)^2}\,\frac{M_{\rm det}}{m_{\rm target}} \approx 200\,f\left(\frac{\rm Mpc}{D_{\rm A}[z]\,(1+z)}\right)^2\,\frac{M_{\rm det}}{1\,{\rm MTon}}\,\frac{10\,{\rm amu}}{m_{\rm target}} \tag{30}$$

where f is the fraction of neutrinos flavors to which it is sensitive, $M_{\rm det}$ is the mass of the detector and $m_{\rm target}$ the mass associated with each target particle. For example a water molecule provides two hydrogen nuclei as inverse beta decay targets only sensitive to $\overline{\nu}_{\rm e}$ and has mass 18 amu so $f \simeq \frac{1}{6}$ and $m_{\rm target} = 9\,{\rm amu}$. If we take a threshold of 5 neutrinos a water Cerenkov detector has distance threshold

$$D_{\rm A}^{\rm range} \approx 3\,{\rm Mpc}\left(\frac{M_{\rm det}}{1\,{\rm MTon}}\right)^{1/2} \tag{31}$$

for $z \ll 1$. So one can't see much further than the next galaxy (Andromeda) with a 1 MTon water detector like the proposed Hyper-Kamiokande [23,24]. Much larger neutrino detector arrays, 10^4 times larger, have been proposed, not for scientific but rather socio-political reasons [25], and could also be used for neutrino astronomy.

Eq. (31) assumes negligible confusion with background events. Both the foreground and background event rates scale linearly with detector mass and for very large detectors the number of SN neutrinos from a distant burst may be large but the number of background events during the burst may be comparable to or larger. When this ratio exceeds unity the threshold distance starts to scale more slowly: $D_{\rm A}^{\rm threshold} \propto M_{\rm det}{}^{1/4}$.

Since the SNe rate increases rapidly with distance, scaling like $D_{\rm A}{}^3$ one can imagine statistically analyzing neutrino counts from SNe more distant than $D_{\rm A}^{\rm range}$. One does not need multiple neutrinos from all the SNe only from some of them to get distance information. Since SN neutrinos are clustered in time while background events are not they are distinguishable and one can glean information about neutrino masses and distances from the statistics of the diffuse supernova neutrino background (DSNB). A companion paper will examine the these issues quantitatively [10].

■ Summary

This paper has examined the use of time delays associated with the mass of ultra-relativistic particles (namely neutrinos) as a probe of space-time geometry. This leads to a new distance measure, the kinematic radial distance, $R_{\rm k}$. This distance is defined in eq. (10) for an arbitrary space-time geometry and it is shown that it is distinct from other measures of distance such as the angular diameter distance, $D_{\rm A}$. It is also shown that for ultra-relativistic particles the proper time-of-flight experienced by the particle carries the same information as $R_{\rm k}$ for arbitrary space-time geometry. Eq. (22) shows how one can combine $R_{\rm k}[z]$ with $D_{\rm A}[z]$ and gravitational lensing shear to measure, along any line-of-sight, one component of the Ricci curvature, which yields one component of the of stress-energy assuming Einstein's equations. In the standard model of cosmology (ΛCDM) we show the component determined is $\rho_{\rm m}$ (the dark matter plus baryon density) but it is shown that for $z \lesssim 1$ determining $\rho_{\rm m}$ requires extremely precise measurements of both $R_{\rm k}[z]$ and $D_{\rm A}[z]$. In fact $R_{\rm k}[z] \cong D_{\rm A}[z]$ to high accuracy, for, $z \lesssim 1$ so one can use one as a surrogate for the other.

We review some practical aspects of measuring R_k in light of recent experimental determinations of neutrino properties. We show that for allowable neutrino masses that the time delays can be larger than the expected length of a neutrino burst from a supernova, and the effect of R_k is readily apparent in the burst profile. In some cases the differential time delay of the different mass eigenstates will lead to significant flavor segregation in the burst. It was argued that within the range of a given neutrino telescope the sensitivity to non-zero R_k is independent of distance. While detecting the effect of finite R_k on SNe neutrino bursts is challenging the current neutrino parameters gives a well defined target for future neutrino telescopes.

Acknowledgments

I would like to thank Chris Kelso, Dan Hooper, Scott Dodelson, John Beacom, and Daniel Holz for many insightful conversations. This work was supported by the DOE at Fermi National Accelerator Laboratory under Contract No. DE-AC02-07CH11359

Footnotes

[a] The $\sigma \propto G_F^2 E_\nu^2$ scaling derives directly from $W^\pm$ or Z^0 boson exchange but neglects kinematic factors which generally suppress the cross-section. Processes like inverse β decay have a threshold (Q) below which the cross-section goes to zero and only achieves the E_ν^2 scaling when $E_\nu - Q \gg m_e$. Neutrino-electron scattering is kinematically suppressed by a factor m_e / E_ν until $E_\nu \gg m_e$. So $\sigma_w \propto G_F^2 E_\nu^2$ really only applies for $E_\nu \gg 1$ MeV, which is true for the bulk of the neutrinos in a SN burst but not to the low energy tail.

[b] One must also be able to determine that the neutrinos detected are from the same SN but this is the same requirement as there being negligible backgrounds.

References

[1] T. Schwetz, M. Tortola, J. Valle *Where we are on θ_{13}: addendum to 'Global neutrino data and recent reactor fluxes: status of three-flavor oscillation parameters* New. J. Phys. **13** (2011) 9401

[2] E. Otten & C. Weinheimer *Neutrino mass limits from tritium β decay* Rep. Prog. Phys. **71** (2008) 086201

[3] A. Melchiorri, S. Dodelson, P. Serra, A. Slosar *New Constraints on Neutrino from Cosmology* New Astro. Rev. **50** (2006) 1020

[4] K. Hirata, *et al*. *Observation of a neutrino burst from the supernova 1987A* Phys. Rev. Lett. **58** (1987) 1490

[5] R. Bionta, *et al*. *Observation of a neutrino burst in coincidence with supernova 1987A in the Large Magellanic Cloud* Phys. Rev. Lett. **58** (1987) 1494

[6] E. Alekseev, L, Alekseev, L. Volchenko, I. Krivoheina *Possible detection of a neutrino signal on 23 February 1987 at the Baksan underground scintillation telescope of the Institute of Nuclear Research* JETP **45** (1987) 589

[7] D. Arnett, J. Bahcall *Supernova 1987a* Ann. Rev. Ast. Astrophys. **27** (1989) 629

[8] H. Janka *et al*. *Theory of core-collapse supernova* Phys. Rep. **442** (2007) 38

[9] G. Zatsepin *Probability of Determining the Upper Limit of the Neutrino Mass from the Time of Flight* JETP **8** (1968) 205

[10] A. Stebbins, C. Kelso, D. Hooper, in preparation

[11] L. Stodolsky *Neutrino flight times in Cosmology* Phys. Lett. B **473** (2000) 61

[12] S. Choubey, S. King *Gamma ray bursts as probes of neutrino mass, quantum gravity and dark energy* Phys. Rev. **D67** (2003) 073005
[13] G. Ellis, S. Nel, R. Maatens, W. Stroeger *Ideal Observational Cosmology* Physics Reports **124** (1985) 315
[14] A. Stebbins *WYSIWYG Space-Time* in preparation
[15] K. Greisen *End to the Cosmic Ray Spectrum* Phys. Rev. Lett. **16** (1966) 748
[16] G. Zatsepin, V. Kuz'min *Upper Limit of the Spectrum of Cosmic Rays* JETPL **4** (1966) 78
[17] S. Weinberg *Gravitation and Cosmology* New York: J. Wiley & Sons (1972) §14.4
[18] S. Webb *Measuring the Universe: The Cosmological Distance Ladder* Chichester: Praxis Publishing (1999)
[19] A. Albrecht *et al*. *Report of the Dark Energy Task Force* arXiv:astro-ph/0609591 (2006)
[20] S. Larson *et al*. *Seven-Year Wilkinson Microwave Anisotropy Probe (WMAP) Observations: Power Spectra and WMAP-Derived Parameters* Astrophys. J. Suppl. **192** (2011) 16
[21] F. An *et al*. *Observation of Electron-Antineutrino Disappearance at Daya Bay* Phys. Rev. Lett. **108** (2012) 171803
[22] G. Bellini *et al*. *Precision Measurement of the* ^{7}Be *Solar Neutrino Interaction Rate* Phys. Rev. Lett. **107** (2011) 141302
[23] N. Kenzo *Hyper-Kamiokande --- a Next Generation Water Cerenkov Detector* in *Neutrinos and Implications for Physics Beyond the Standard Model*; ed. R. Shrock. Singapore: World Scientific (2003) 307
[24] K. Abe *Letter of Intent: The Hyper-Kamiokande Experiment --- Detector Design and Physics Potential* --- arXiv1109.3262 (2011)
[25] J. Learned *Reactor Monitoring (near and far) with Neutrinos* Nucl. Phys. B Suppl. **143** (2005) 152

Figures

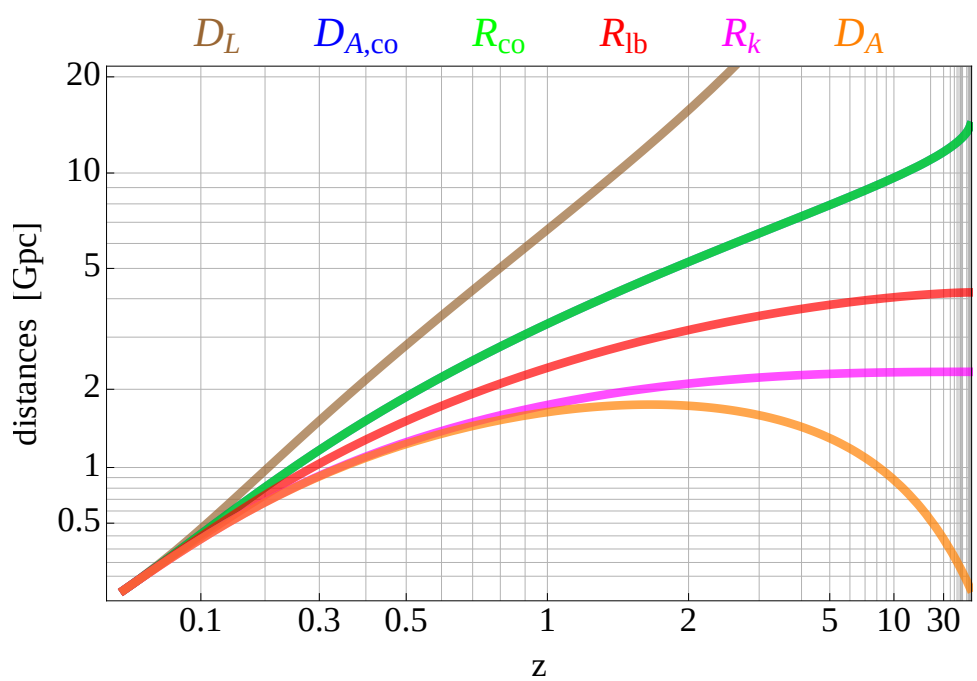

Figure 1. Plotted are five measures of distance for a concordance cosmology as a function of redshift. From top to bottom these are the bolometric luminosity distance, the comoving radial distance, the lookback distance, the kinetic radial distance, and the angular diameter distance. The comoving angular diameter distance is obscured by the comoving radial distance because this concordance model is flat ($\Omega_0 = 1$) so $D_{A,\mathrm{co}}[z] = R_{\mathrm{co}}[z]$.

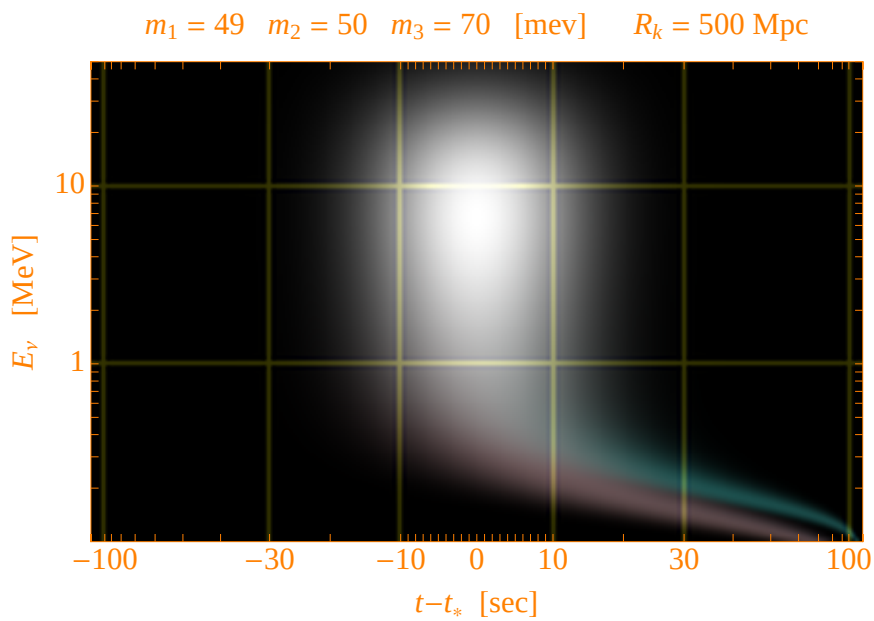

Figure 2. Plotted is a (idealized) neutrino burst profile as would be observed from a SN at $R_k = 500$ Mpc away. It is assumed that each flavor of neutrino was emitted with the same $T = 6$ MeV Fermi-Dirac spectrum releasing a total energy of 3×10^{53}ergs spread over a Gaussian time window such that half the neutrinos are emitted in a 7sec interval in the SN rest frame. The RGB color, plotted as a function of time and energy, is proportional to the cube root of the neutrino flux in particles per unit time per unit energy (the cube root is used to increase the contrast) for electron (R), muon (G), and tau (B) neutrinos. The colors are normalized to pure white at burst maximum. The best fit mixing angles and differences in mass squared are used, the normal mass hierarchy ($m_1 < m_2 < m_3$) is assumed, as is $\sum_{i=1}^{3} m_i = 0.17\,\mathrm{eV}/c^2$ corresponding the most stringent cosmological limit at this time. Most notable is the low energy tail which swings to the right due to the time delays which increase with decreasing energy. The difference in the mass eigenstates causes this tail to be split in three but only two tails are discernible corresponding to mass splitting between m_1, m_2 and m_3. The smaller m_1-m_2 mass splitting is washed out by the relatively long duration of the burst. The reddish tail is a mixture of $m_1$and m_2 and carries 2/3rds of the neutrinos in the tail while the blue-green tail is from the m_3 and carries 1/3rd of the tail. Electron neutrinos which interact with normal matter through a charged current are predominantly in the red tail, while the other flavors including those in the blue-green tail can interact through neutral currents. The time splitting between the two tails is fully determined by current measurements of mass splittings, but the overall swing of the tail is determined by the currently unknown absolute mass scale of the neutrino mass hierarchy.

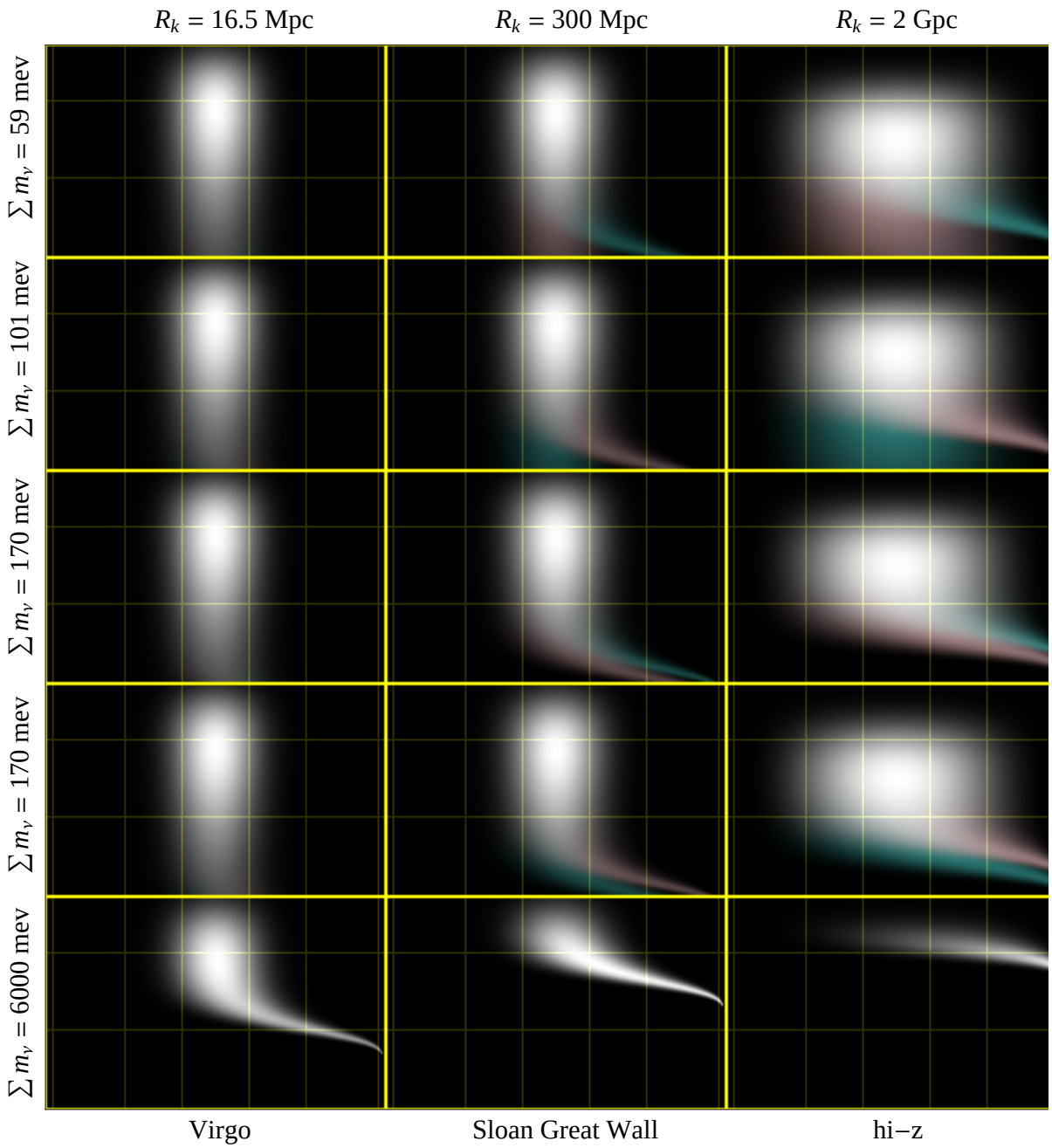

Figure 3. An array of plots like figure 2 with same energy and time scale but for a variety of distances and absolute neutrino mass scales. The left column is for SNe at a distance corresponding to the nearest concentration of galaxies, the middle is at the distance of the largest known notable feature in the distribution of galaxies, and the left for z $\gtrsim$ 1. Both the normal ($m_1 < m_2 < m_3$) and inverted ($m_3 < m_1 < m_2$) mass hierarchies are considered. Note that the order of the red and blue-green tail are reversed between normal and inverted mass hierarchies but the time splitting is the same. The top two rows are for the minimal absolute mass scale allowed by current observations. This mass scale is roughly the sensitivity of the upcoming KATRIN experiment. The middle two rows are for the maximum absolute mass scale allowed by the most stringent published cosmological limits. The bottom row is for the maximum absolute mass scale allowed by current

laboratory limits.